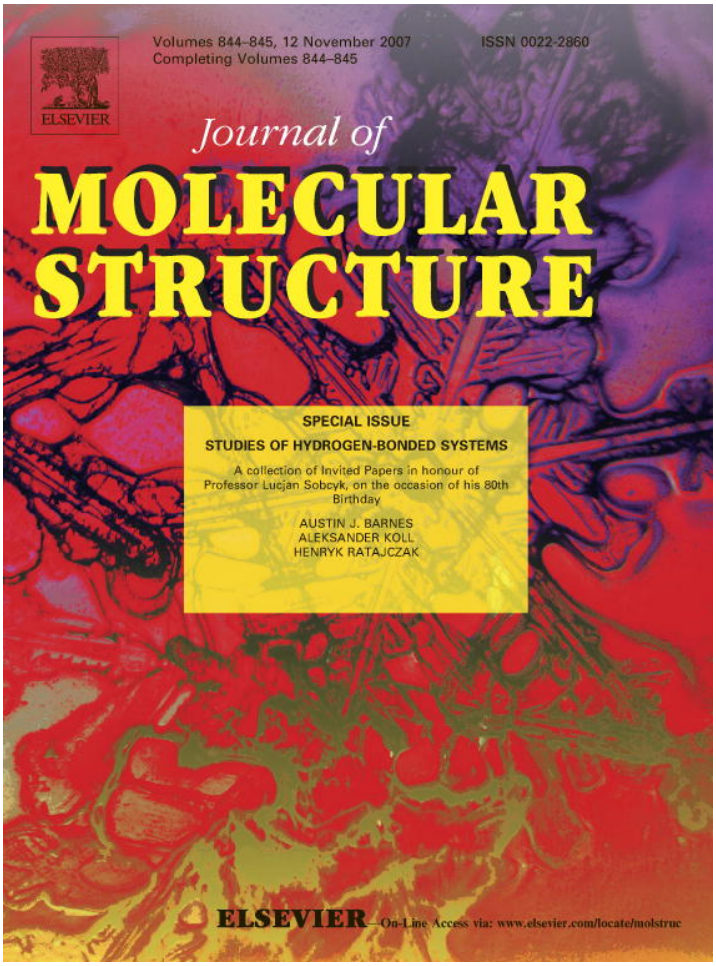

Available online at www.sciencedirect.com
ScienceDirect
Journal of Molecular Structure 844–845 (2007) 319–327
Journal of MOLECULAR STRUCTURE
www.elsevier.com/locate/molstruc

Observation by NMR of the tautomerism of an intramolecular OHOHN-charge relay chain in a model Schiff base

Nikolai S. Golubev [a], Sergei N. Smirnov [a], Peter M. Tolstoy [a,b,*], Shasad Sharif [b], Michael D. Toney [c], Gleb S. Denisov [a], Hans Heinrich Limbach [b]

[a] *V.A. Fock Institute of Physics, St. Petersburg State University, Russia*
[b] *Institute of Chemistry, Free University of Berlin, Germany*
[c] *Department of Chemistry, University of California, Davis, USA*

Received 23 March 2007; received in revised form 12 April 2007; accepted 13 April 2007
Available online 20 April 2007

Dedicated to Prof. Lucjan Sobczyk on the occasion of his 80th birthday.

Abstract

As a model system for the internal and external aldimines of the coenzyme pyridoxal phosphate (PLP) in PLP dependent enzymes we have studied the ^{1}H and ^{15}N NMR spectra of the ^{15}N labeled Schiff base 3-carboxy-5-methyl-salicylidenaniline (**1**) dissolved in CD_2Cl_2. **1** contains a charge relay system with two strongly coupled intramolecular hydrogen bonds of the OHOHN type. One-bond $^{15}N—^{1}H$ scalar spin–spin coupling constants and chemical shifts of partially deuterated **1** were measured in the temperature range between 243 and 183 K and analyzed assuming an exchange between three tautomeric states exhibiting well defined hydrogen bond geometries. The analysis shows that the dominant structure **1b** corresponds to the zwitterion $O—H\cdots O^{-}\cdots H—N^{+}$, where deuteration of one bond leads to a shortening of the other. This anti-cooperative effect is revealed by the vicinal isotope effects on the proton chemical shifts. By contrast, forms **1a** and **1c** are characterized by the structures $O—H\cdots O—H\cdots N$ and $O^{-}\cdots H—O\cdots H—N^{+}$, correspondingly, whose hydrogen bonds exhibit a cooperative coupling. We predict that **1a** will dominate at high temperatures and low dielectric constants, whereas **1c** will dominate at low temperatures and large dielectric constants. The comparison with model systems which do not contain the additional COOH-group indicates that the latter is responsible for the dominance of the zwitterionic structure of the OHN hydrogen bond. The implications of these findings for the function of the coenzyme pyridoxal phosphate in its natural environment are discussed.

Keywords: Charge relay chain; Hydrogen bond; Schiff base; Tautomerism; Low temperature NMR; Isotope effect

1. Introduction

Pyridoxal phosphate (PLP, vitamin B_6) is found in the active sites of many enzymes where it forms a Schiff base to a lysine side chain (Fig. 1) or to a free amino acid which is going to be transformed. The first is called "internal" and the second "external" aldimine [1–5]. The aldimines exhibit an intermolecular low-barrier OHN hydrogen bond between an aspartate residue and the pyridine ring which has been modeled by NMR using pyridine–carboxylic acid complexes [6–9]. Essential is also an intramolecular OHN hydrogen bond between the phenolic OH group and the imino nitrogen. For model Schiff bases tautomeric equilibria between an $O—H\cdots N$ and an $O^{-}\cdots H—N^{+}$ forms (see Fig. 2) have been established for liquid solutions [10,11]. It has been argued that these fast equilibria are pre-requisite for the enzymatic activity [12]. The equilibria were studied by UV–Vis [13] and NMR [14–17] spectroscopy. Many factors, such a temperature, solvent polarity and chemical substitution in the molecule influence the equilibrium. The

* Corresponding author. Address: Institute of Chemistry, Free University of Berlin, Germany. Tel.: +49 30 8385 3615; fax: +49 30 8385 5310.
E-mail address: tolstoy@chemie.fu-berlin.de (P.M. Tolstoy).

0022-2860/$ - see front matter © 2007 Published by Elsevier B.V.
doi:10.1016/j.molstruc.2007.04.015

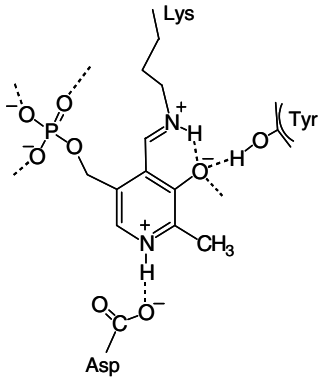

Fig. 1. Fragment of the active site of aspartate aminotransferase; PLP cofactor with additional hydrogen bonding to the side chain of neighbouring amino acid is shown.

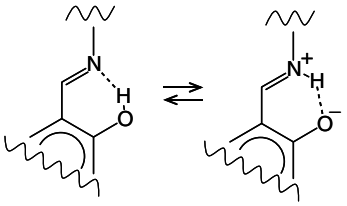

Fig. 2. Common structural element of the PLP-like Schiff bases. Tautomerism between a molecular O—H···N form and a zwitterionic $O^{-}\cdots H{-}N^{+}$ form is shown.

typical range of differences in enthalpy ΔH and entropy ΔS between OH- and NH-forms for alkyl-substituted Schiff bases are from -7 to $-13\ \mathrm{kJ\,mol^{-1}}$ and from -30 to $-50\ \mathrm{J\,mol^{-1}\,K^{-1}}$, respectively, and the equilibrium shifts significantly with the temperature [15,18]. For phenyl-substituted Schiff bases, the OH-form predominates and the equilibrium shifts only slightly with temperature [19,20]. Additional intermolecular OHO hydrogen bonding to the phenolic oxygen has been studied previously by NMR spectroscopy [9]. It has been demonstrated that additional bonding increases the acidity of the hydroxyl and shifts the equilibrium to the NH-form of the Schiff base.

Both the inter- and the intramolecular hydrogen bonds are coupled in the sense that a proton shift towards the ring nitrogen also favours the zwitterionic form of the intramolecular OHN hydrogen bond [9,21]. Coupled hydrogen bonds exhibiting the property of rapidly moving electrical charges via a coupled proton transfers have also been called "charge relay chains" [22].

In previous papers it has been shown for carboxylic acid–pyridine complexes that intrinsic changes of NMR parameters with temperature may occur which arise from temperature dependent solute–solvent interactions and hence temperature dependent hydrogen bond geometries averaged over various solvent configurations [23] called "solvatomers" by Perrin and Lau [24]. Such geometric changes have been analyzed in terms of hydrogen bond correlation techniques [25]. According to the latter, the A···H and the H···B distances in AHB hydrogen bond are correlated in the sense that when H is transferred from A towards B, the AB distance decreases to a minimum for the quasi-symmetric complex and then increases again.

Often, NMR parameters of the nuclei in hydrogen bridges are also correlated with the hydrogen bond geometries [26]. Thus, it is possible to obtain information about hydrogen bond geometries in liquids by NMR. Unfortunately, in order to exploit very high resolution of NMR for hydrogen bonded systems one needs to perform difficult low temperature experiments in order to observe individual hydrogen bonds in the slow hydrogen bond exchange regime [21]. Such experiments often fail because of a low solubility of the target compound. Therefore, inspired by PLP, we have focussed on 3-carboxy-5-methyl-salicylidenaniline (**1**) (Fig. 3a) which represents an intramolecular charge relay chain. Here, the geometries of both hydrogen bonds can potentially be studied in a larger temperature interval using liquid state NMR techniques. **1** exhibits potentially three different tautomeric states **1a**–**1c** as depicted in Fig. 3a (Fig. 3b will be discussed later). Our goal was to characterize these tautomers and their equilibria in more detail by measuring different NMR parameters.

The most important parameter we have measured was the one-bond $^{1}J(^{15}\mathrm{N},^{1}\mathrm{H})$ scalar coupling constant which can give direct information about the tautomerism of OHN hydrogen bond [27–29]. For that purpose we have labeled **1** with the ^{15}N isotope. Unfortunately, $^{1}J(^{15}\mathrm{N},^{1}\mathrm{H})$ scalar couplings are rather insensitive to the interconversion between **1b** and **1c**, because in this process the NH distance does not change significantly. Therefore, besides measurements of the chemical shifts of hydrogen bonded protons in **1**, we have measured the effect on the ^{1}H chemical shift of a given H-bond arising from substitution of H for D in the neighbouring hydrogen bond. Such "vicinal" or "long-range" isotope effects can be used to establish the mutual coupling scheme of two interacting hydrogen bonds [30,31]. If the neighbouring hydrogen bonds are cooperatively arranged as in AH···AH···B or $A^{-}\cdots HA\cdots HB^{+}$, deuteration of one of them will lead to the lengthening of the other one and corresponding shielding of the neighbouring bridging proton. In contrast, if hydrogen bonds are anti-cooperatively arranged as in $AH\cdots A^{-}\cdots HB^{+}$, deuteration will lead to shortening of the other hydrogen bond and corresponding deshielding of its bridging proton.

2. Experimental

3-Carboxy-5-methyl-salicylidenaniline was synthesised from 3-carboxy-5-methyl-salicylaldehyde and aniline-^{15}N (96% of ^{15}N isotope) using standard techniques for Schiff base synthesis [32]. The aldehyde–acid precursor was obtained via the formylation of 5-methylsalicylic acid by chloroform in alkali media, according to the Reimer–Tiemann reaction [33]. Deuteration of the Schiff base was accomplished by repeated re-crystallization from methanol-OD. The total deuterium fraction was determined by comparison of the integrated signal intensity of the residual

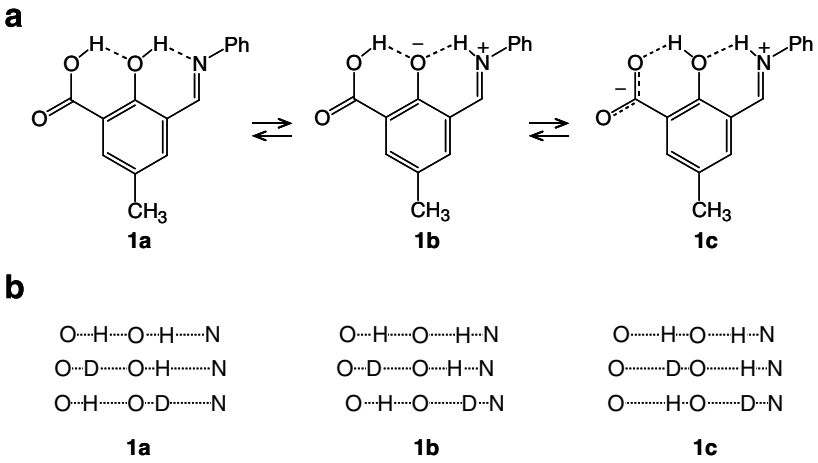

Fig. 3. (a) Possible tautomeric structures of 3-carboxy-5-methyl-salicylidenaniline (**1**). (b) Vicinal H/D isotope effects on the hydrogen bond geometry; cooperatively coupled hydrogen bonds in **1a** and **1c**; anti-cooperatively coupled hydrogen bonds in **1b**.

mobile proton NMR signal with those of the immobile CH-protons. The relatively low deuteration ratios obtained in this work are due to the H/D exchange between **1** and the moisture during the handling of the substance, as well as due to proton exchange between **1** and traces of water in the NMR sample. NMR spectra were obtained on a Bruker DPX-300 spectrometer in the temperature range 243–183 K using CD_2Cl_2 as solvent. The chemical shifts of ^{15}N nuclei were measured with respect to nitromethane as an internal standard and then re-calibrated to the NH_4Cl scale. The absolute concentration of the samples was approximately 0.01 M for ^1H NMR and approximately 0.05 M for ^{15}N NMR measurement.

3. Results

The NMR signals of the hydrogen bond protons and of the Schiff base nitrogen of **1** dissolved in CD_2Cl_2, recorded at 233 K are depicted in Fig. 4. The nitrogen signal was obtained in the absence of ^1H decoupling. The molecules of **1** were partially deuterated in the mobile proton sites; the deuterium fraction x_D was approximately 0.2. The assignment of the signals to the individual isotopologs OHOHN, ODOHN and OHODN was accomplished by comparison of the experimental line intensities with those predicted for a statistical distribution of the isotopologs. The δ(O*H*OHN) and δ(O*H*ODN) signals are singlets. The δ(OHO*H*N) and δ(ODO*H*N) signals exhibit a doublet of doublets due to scalar spin–spin coupling with ^{15}N and the nearest CH proton. The ^{15}N NMR signal consists of several subsignals. The δ(OHOH*N*) and δ(ODOH*N*) signals are split into doublets and the δ(OHOD*N*) signal into a triplet. At $x_D = 0.2$ the concentration of ODODN is too small to give rise to an observable nitrogen signal. By the line shape analysis the values of the coupling constants $^1J(\mathrm{OHO}^1H^{15}N) \equiv J(\mathrm{OHO}HN)$ and $^1J(\mathrm{ODO}^1H^{15}N) \equiv J(\mathrm{ODO}HN)$ are obtained, which are negative because of the negative gyromagnetic ratio of ^{15}N. For convenience, we omit the sign as it cannot be directly determined from the spectra. The ^1H and ^{15}N NMR parameters obtained from Fig. 4 are listed in Table 1. They will be discussed later.

Temperature dependent ^1H NMR spectra were recorded in the temperature range from 183 to 243 K and are shown in Fig. 5. At temperatures higher than 243 K intermolecular proton exchange significantly broadens the lines. The assignment of the peaks follows that of Fig. 4. The ^1H NMR parameters for all temperatures are collected in Table 2.

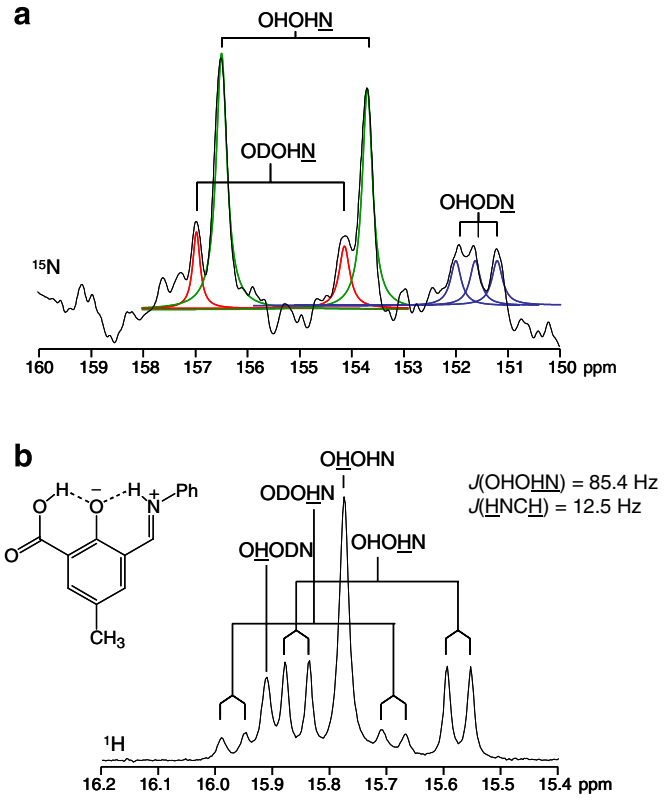

Fig. 4. ^{15}N (a) and ^1H (b) NMR spectra of the solution, containing 0.05 M of **1** (96% ^{15}N, $x_D = 0.2$) at 233 K in CD_2Cl_2. Isotopolog ODODN is not seen in ^{15}N spectrum due to the low deuteration ratio x_D.

Table 1
NMR spectroscopic parameters of intramolecular hydrogen bonds for solution of **1** in CD_2Cl_2 at 233 K

δ(O*H*OHN) ± 0.005 (ppm)	15.774
δ(O*H*ODN) ± 0.005 (ppm)	15.911
δ(O*H*ODN) − δ(O*H*OHN) ± 0.007 (ppm)	+0.137
δ(OHO*H*N) ± 0.005 (ppm)	15.714
δ(ODO*H*N) ± 0.005 (ppm)	15.826
δ(ODO*H*N) − δ(OHO*H*N) ± 0.007 (ppm)	+0.112
δ(OHOH*N*) ± 0.05 (ppm)	155.09
δ(OHOD*N*) ± 0.05 (ppm)	151.57
δ(OHOD*N*) − δ(OHOH*N*) ± 0.07 (ppm)	−3.52
δ(ODOH*N*) ± 0.05 (ppm)	155.55
δ(ODOH*N*) − δ(OHOH*N*) ± 0.07 (ppm)	+0.46
J(OHO*HN*) ± 0.5 (Hz)	85.4
J(ODO*HN*) ± 0.5 (Hz)	84.6
J(ODO*HN*) − J(OHO*HN*) ± 0.7 (Hz)	−0.8
J(*H*CN*H*) ± 0.5 (Hz)	12.5

^{15}N NMR chemical shifts are referenced to NH_4Cl.

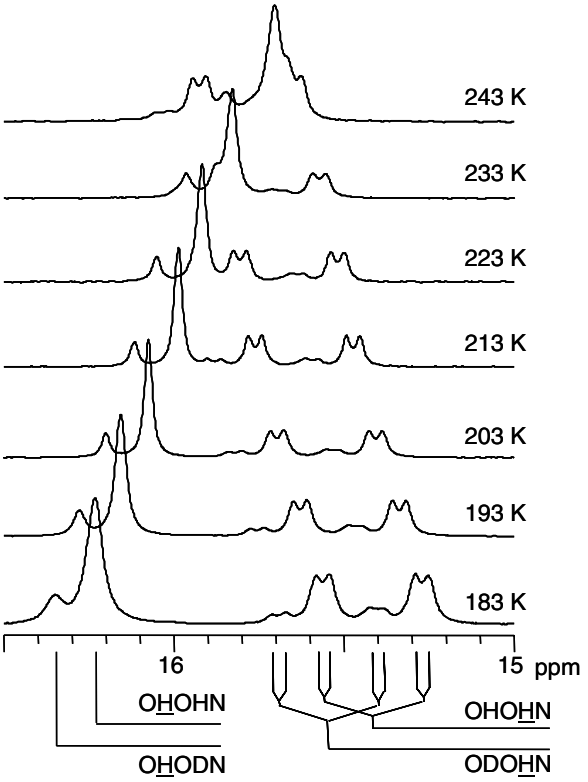

Fig. 5. ^{1}H NMR spectra of the solution, containing 0.01 M of **1** (96% ^{15}N, $x_D = 0.2$) in CD_2Cl_2 in the temperature range 183–243 K.

4. Discussion

In the previous section, we have described the ^{1}H and ^{15}N NMR spectra of ^{15}N enriched **1** dissolved in CD_2Cl_2 in the temperature range between 243 and 183 K. In this section we will analyze these parameters in order to derive information about the hydrogen bond geometries and proton transfer mechanisms in this compound.

4.1. General discussion of NMR parameters

The analysis of the NMR parameters strongly depends on whether they represent averages over the different tautomeric forms of Fig. 3a or whether single structures are present exhibiting temperature dependent hydrogen bond geometries. In order to answer this question we have plotted in Fig. 6a correlation established previously between the two natural hydrogen bond coordinates $q_1 = 1/2$ $(r_1 - r_2)$ and $q_2 = r_1 + r_2$ of OHN hydrogen bonds where r_1 and r_2 are distances from the proton to the oxygen and nitrogen atoms, correspondingly [7,25,34]. The dashed curve refers to equilibrium geometries whereas the dotted line includes an empirical correction for zero-point vibrations [7]. Similar correlations have been observed for OHO and NHN hydrogen bonds [35–37]. The geometries of low-barrier or no-barrier hydrogen bonds correspond to the points on the correlation curve. Generally, it has been observed that lowering the temperature and increasing of the dielectric constants compresses an O—H···N hydrogen bridge and widens a zwitterionic $O^-\cdots H{-}N^+$ bridge [23], corresponding to intersection points 1–4 on the left and on the right side of the correlation curve in Fig. 6a. The lines connecting these intersection points represent then the average geometries in the presence of a tautomerism between a molecular O—H···N form and a zwitterionic $O^-\cdots H{-}N^+$ form. At the left and right intersection points the equilibrium constants of the tautomerism are $K = 0$ and $K \to \infty$, correspondingly. The parameters used to calculate these lines were typical for six-membered intramolecular OHN hydrogen bonded cycle in Schiff bases [21]. Line 1 refers to higher temperatures and lower dielectric constants whereas line 4 refers to lower temperatures and larger dielectric constants. These lines were estimated from the ^{1}H *vs.* ^{15}N chemical shift correlation for intramolecular OHN hydrogen bonds of Schiff bases [9] depicted in Fig. 6b. The dotted curve was estimated for low-barrier or no-barrier hydrogen bonds exhibiting a sequence of protonation states where H is shifted from oxygen to nitrogen. The solid straight lines now refer to the average ^{1}H/^{15}N chemical shifts in the presence of a tautomerism between a O—H···N form and a $O^-\cdots H{-}N^+$ form.

The data point symbolized by the filled circle in Fig. 6b was obtained in this study for **1** in CD_2Cl_2 at 233 K. Clearly, the data point is not located on the correlation curve but on line 2. This finding is a strong indication of the presence of a OHN tautomerism in **1**. For similar temperatures and the same solvent, however, we would have expected for OHN hydrogen bonds of phenyl-substituted Schiff bases chemical shifts and geometries as represented by the open circles in Fig. 6 [9]. We associate this change to the presence of the carboxylic group in **1**, which increases the acidity of the hydroxyl and strongly shifts the equilibrium between molecular OH···N and zwitterionic $O^-\cdots HN^+$ forms towards the latter.

Table 2
^{1}H NMR spectroscopic parameters of intramolecular hydrogen bonds for solution of **1** in CD_2Cl_2 at various temperatures

T (K)	δ(O*H*OHN) (ppm)	δ(O*H*ODN) (ppm)	δ(OHO*H*N) (ppm)	δ(ODO*H*N) (ppm)	J(OHO*HN*) (Hz)
243	15.705	15.870	15.820	15.940	84.3
233	15.812	15.965	15.720	15.849	85.0
223	15.910	16.063	15.649	15.780	85.8
213	16.002	16.138	15.575	15.709	86.3
203	16.084	16.211	15.501	15.643	86.9
193	16.152	16.268	15.457	15.596	87.3
183	16.224	16.322	15.409	15.551	87.8

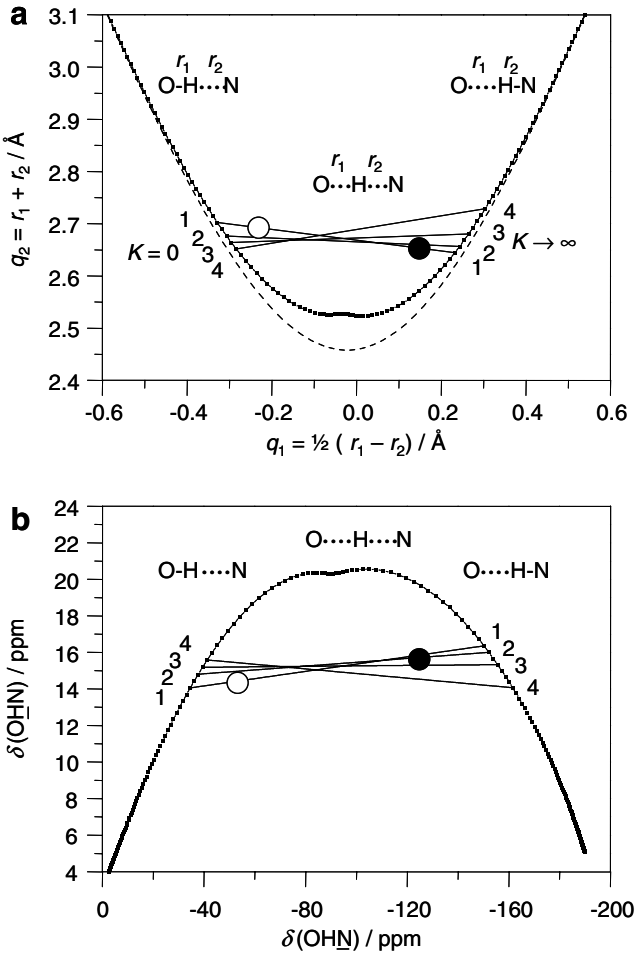

Fig. 6. Hydrogen bond correlation of OHN hydrogen bonds. (a) Geometric OHN hydrogen bond correlation of $q_2 = r_1 + r_2$ as a function of $q_1 = 1/2(r_1 - r_2)$, where r_1 and r_2 are distances from the bridging proton to the heavy atoms, according to Ref. [7]. (b) ^{1}H *vs.* ^{15}N chemical shift correlation of Schiff bases exhibiting an intramolecular OHN hydrogen bond and a tautomerism between a molecular O—H···N and a zwitterionic $O^-\cdots H{-}N^+$ forms. Adapted from Ref. [9]. The full circle refers to **1** dissolved in CD_2Cl_2 at 233 K. The open circle refers to the typical hydrogen bond properties of phenyl-substituted Schiff bases dissolved in CD_2Cl_2. For further description, see text.

4.2. Tautomeric equilibrium model

Whereas Schiff bases studied previously exhibited only a single OHN hydrogen bond, we need to take the OHO hydrogen bond of **1** into account, i.e. three tautomeric states according to Fig. 3a are needed in order to describe the dependence of the NMR parameters assembled in Table 2 on temperature. For a given parameter P such as a chemical shift or a coupling constant it follows that

$$P_{\text{obs}} = x_a P_a + x_b P_b + x_c P_c, \quad (1)$$

where x_i represents the mole fraction of the tautomeric state i and P_i represents its intrinsic but temperature dependent chemical shift or coupling constant; $i = a, b, c$. The mole fractions x_i depend in the usual way on the equilibrium constants K_{ab} and K_{bc} of the two tautomeric equilibria as illustrated in Fig. 7. These constants can be different for the different isotopologs of **1**. Thus, each NMR parameter measured depends on the three intrinsic parameters of the three forms and on two equilibrium constants. The number of parameters represents a problem for the fitting as measurements could be done only in a limited temperature range because of the low solubility of **1**.

Nevertheless, we have plotted in Fig. 8 the average NMR parameters of Table 2 as a function of temperature and added the solid curves calculated using Eq. (1) and a parameter set which was obtained as follows. Firstly, we have neglected any isotope effect on the equilibrium constants, i.e. set

$$K_{ab}^{\text{HH}} = K_{ab}^{\text{HD}} = K_{ab}^{\text{DH}} = \exp(\Delta S_{ab}/R)\exp(-\Delta H_{ab}/RT) \text{ and} \quad (2)$$
$$K_{bc}^{\text{HH}} = K_{bc}^{\text{HD}} = K_{bc}^{\text{DH}} = \exp(\Delta S_{bc}/R)\exp(-\Delta H_{bc}/RT), \quad (3)$$

where ΔH_{ij} and ΔS_{ij} represent the reaction enthalpy and entropy of the interconversion between tautomeric states i and j in Fig. 7. Though the isotope effects on equilibrium constant can often be well pronounced [34b], this simplification is in agreement with previous findings for a model Schiff base [21]. The vicinal H/D isotope effects on the chemical shift of a given hydrogen bonded proton observed were then associated with changes of the intrinsic values after deuteration in the neighbouring site rather than with changes of equilibrium constant. This type of isotope effect has been called "equilibrium averaged intrinsic isotope effect" [21]. Secondly, we have assumed a preliminary set of NMR and thermodynamic parameters for the structures **1a**–**1c**. Using these parameters we have calculated the analytical curves for the temperature dependencies of the mole fractions and of the averaged NMR parameters. Finally, we have adjusted the parameters in order to fit analytical curves to the experimental points (see solid lines in Fig. 8). As a result, we got a "reasonable" but somewhat

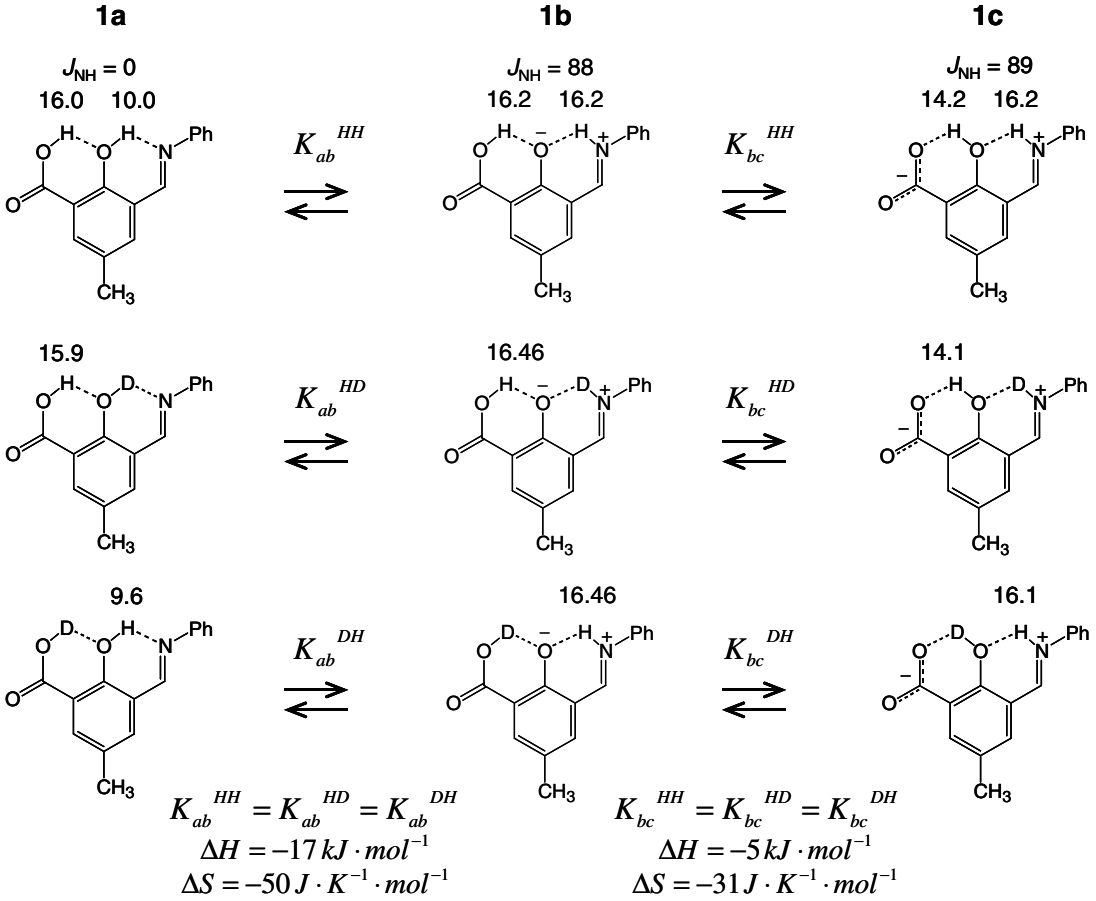

Fig. 7. Equilibrium constants of tautomeric reactions of proton transfer for three isotopologs of **1**. Numbers above the structures represent the fitted intrinsic NMR parameters of the tautomers. Chemical shifts are given in ppm and coupling constants are given in Hz. For more details, see text.

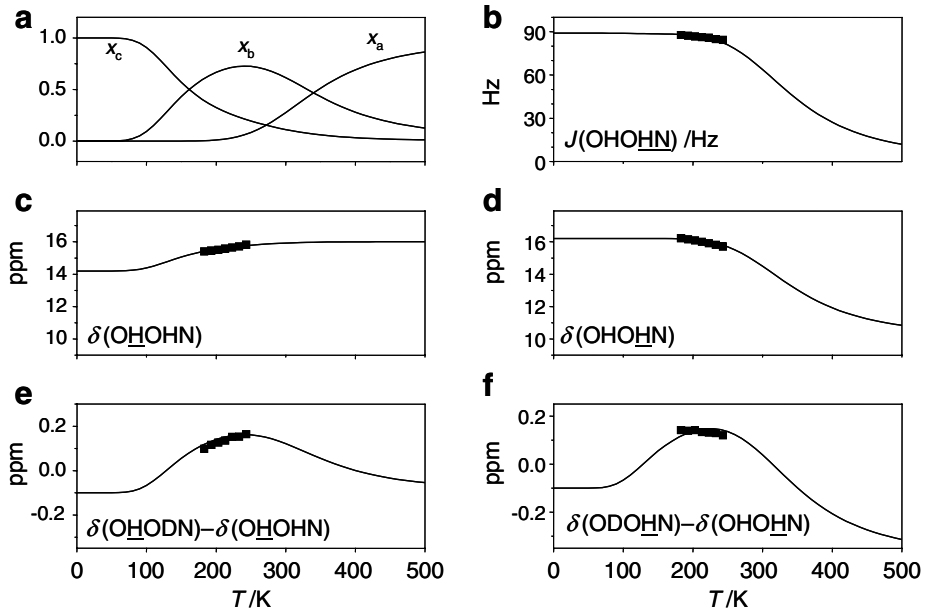

Fig. 8. Temperature dependencies of the observed NMR parameters and of the mole fractions of tautomers of **1**. (a) Mole fractions of **1a**, **1b** and **1c**. (b) Coupling constants J(OHO*H*N). (c) Hydrogen bonding proton chemical shifts δ(O*H*OHN). (d) Hydrogen bonding proton chemical shifts δ(OHO*H*N). (e) Vicinal isotope effects δ(O*H*ODN) − δ(O*H*OHN). (f) Vicinal isotope effects δ(ODO*H*N) − δ(OHO*H*N). Solid lines are calculated using the three-state tautomeric equilibrium model as described in the text.

arbitrary set of intrinsic coupling constants and chemical shifts, which had to be assumed to be independent of temperature. This set can describe well the experimental data, but which is not a unique set and also not a set exhibiting the best agreement with the experiment. All fitted parameters used to calculate the solid curves in Fig. 8 are included in Fig. 7.

Let us now discuss Fig. 8 in more detail. In Fig. 8a, we have plotted the calculated mole fractions of the tautomers **1a**, **1b** and **1c** as a function of temperature. Our choice of reaction enthalpies and entropies leads to a preference of tautomer **1c** at lower temperatures. This choice is justified because **1c** exhibits the largest dipole moment of the tautomeric states in Fig. 7 and structures with large dipole moments are preferred in polar solvents at low temperatures [23,27,38–40]. When temperature is increased, tautomer **1b** and eventually tautomer **1a** are formed.

In Fig. 8b, we have plotted the coupling constants J(OHO*H*N) of **1** as a function of temperature. They are close to 90 Hz at lowest temperatures and decrease slightly with increasing temperature because of the formation of **1a** which exhibits a much smaller coupling constant as compared to the zwitterionic structures **1b** and **1c**.

Figs. 8c and d refer to the chemical shifts δ(O*H*OHN) and δ(OHO*H*N). Their temperature dependence can be explained as follows. The OHO hydrogen bridges in **1a** and **1b** exhibit similar proton chemical shifts, while the OHO bridge in **1c** is somewhat longer and bridging proton is more shielded. In contrast, the OHN bridges in **1b** and **1c** are shorter than in **1a**; therefore, the observed chemical shift δ(OHO*H*N) decreases when temperature increases. The hydrogen bond geometries for OHOHN isotopologs of structures **1a**–**1c** are qualitatively depicted in Fig. 3b.

Fig. 8e shows that the observed vicinal isotope effect δ(O*H*ODN) − δ(O*H*OHN) increases with increasing temperature. This behaviour can be explained as follows. In forms **1a** and **1c** OHO and OHN hydrogen bonds are cooperatively coupled. This means that lengthening of a given bond by its deuteration leads to the lengthening of the other, as illustrated in Fig. 3b. The latter, in turn, is observed in a proton NMR as a negative value of the vicinal isotope effect on bridging proton chemical shift. In contrast, in tautomer **1b** hydrogen bonds are anti-cooperatively coupled (they compete for the central phenolic oxygen). Lengthening of a given hydrogen bond by its deuteration leads to the shortening of the neighbouring one and, consequently, to the deshielding of the bridging proton. Thus, the vicinal isotope effect δ(O*H*ODN) − δ(O*H*OHN) in form **1b** is positive. In the temperature range between 183 and 243 K the mole fraction of **1b** grows and so does the value of the δ(O*H*ODN) − δ(O*H*OHN) isotope effect.

In Fig. 8f, we have plotted the values of δ(ODO*H*N) − δ(OHO*H*N) isotope effect. Similar reasoning as in case of (O*H*ODN) − δ(O*H*OHN) isotope effect is valid. The geometric isotope effects are illustrated in Fig. 3b as well. However, in order to reproduce the decrease of δ(ODO*H*N) − δ(OHO*H*N) with temperature increase we had to use a relatively large negative intrinsic value for **1a**.

In summary, it was possible to explain the experimental data in terms of a tautomerism between the three states in

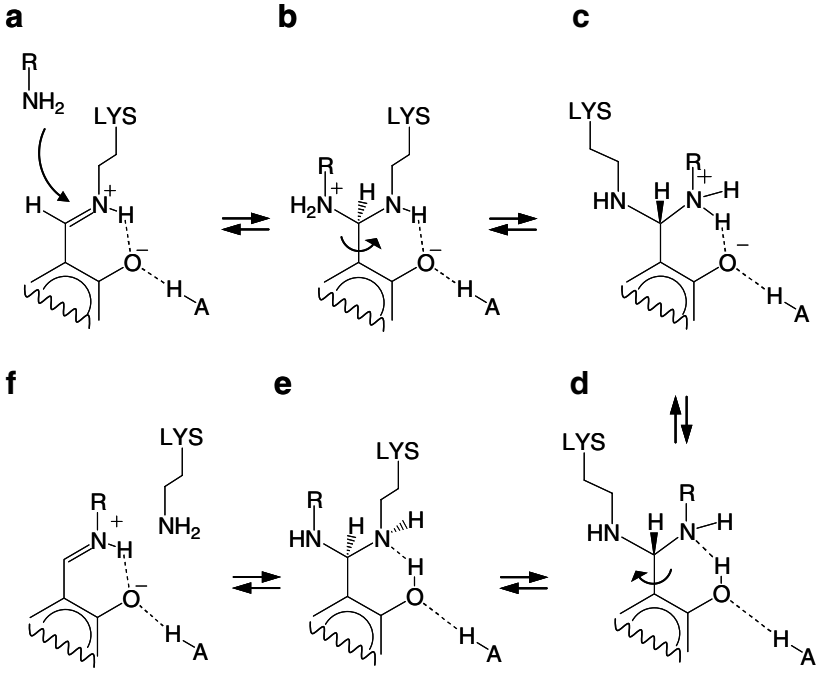

Fig. 9. Potential mechanism of the transimination of the internal aldimine of PLP to the external aldimine, involving geminal diamines as intermediate steps. For further explanation, see text.

Fig. 7. The data are mainly determined by the intrinsic NMR parameters for the dominating tautomer **1b**, but in order to describe the dependence of the data on temperature tautomers **1a** and **1c** cannot be neglected. The set of thermodynamic data and of the intrinsic NMR parameters is only semi-quantitative for which measurements in a larger temperature interval would be required.

4.3. Biological role of additional hydrogen bonds to PLP

The question arises whether the above hydrogen bond assisted intramolecular tautomerism of **1** has some implications for the biological function of the cofactor PLP. Let us remind that PLP dependent enzyme mechanisms uniformly entail transimination to generate the obligatory external aldimine intermediate from the internal aldimine [41,42]. This process could either proceed with or without the assistance of water molecules or additional bases, a problem which is still under debate. A mechanism involving no water molecule is depicted in Fig. 9. The enzyme has prepared the transimination by deprotonation of the amino group of the amino acid RNH_2, by protonation of the pyridine ring and hence of the Schiff base nitrogen (Fig. 9a) [9,21,43]. Here, additional hydrogen bonds to other amino acid residues AH assist this double proton shift as indicated in model studies [21]. This leads to a positive charge on the α-carbon which allows the amino acid to perform the nucleophilic attack on the internal aldimine (Fig. 9a) leading to a geminal diamine. The structures of Figs. 9b and c have been discussed [44] which interconvert by C—C bond rotation and hydrogen bond reorganization. We propose here a subsequent proton transfer to oxygen leading to the structures of Fig. 9d. This could be associated with a weakening or opening of the additional hydrogen bond to the donor AH. Now reverse processes easily lead to the external aldimine shown in Fig. 9f.

We speculate that nature did not select an additional intramolecular hydrogen bond as in **1** because this bond has to be flexible enough in order to allow for the transimination to occur. By contrast, the OHO hydrogen bond of **1** does not open easily. Nevertheless the system represents an interesting model for future theoretical studies which can mimic the effect of the additional H-bonds on the characteristics of the tautomerism on the OHN hydrogen bond.

5. Conclusions

There are several conclusions arising from the findings described above. The first is that the $^{1}H—^{15}N$ hydrogen bond correlation depicted in Fig. 6 allows one to distinguish a low-barrier OHN hydrogen bond from an OHN hydrogen bond exhibiting a tautomerism, i.e. a medium barrier for proton transfer. The second conclusion is that the measurement of vicinal isotope effects allowed us to identify **1b** as main dominant structure. Unfortunately, the temperature interval accessible was too small to obtain all thermodynamic and NMR parameters of the three-state tautomerism of **1**, depicted in Fig. 3a. It would be worth to replace the phenyl ring by other groups which increase the solubility and hence allow one to perform measurements at low temperatures using deuterated freons as solvents. The third conclusion is that we could successfully describe the temperature dependence of the NMR parameters neglecting equilibrium isotope effects on the tautomerism. In other words, the temperature dependence of the vicinal isotope effects on the chemical shifts arises mainly from "equilibrium averaged intrinsic isotope effects" as proposed previously [21]. Finally, already now one may understand why nature did not convert the methyl group of PLP in 2-position into a carboxylic group: the additional hydrogen bond would be too strong and not flexible enough to allow the reaction sequence depicted in Fig. 9. This sequence might be a good starting point for future experimental and theoretical studies.

Acknowledgements

This study has been supported by the Russian Foundation of Basic Research, Grant 05-03-33235, the Deutsche Forschungsgemeinschaft, Bonn and the Fonds der Chemischen Industrie, Frankfurt.

References

[1] A.E. Evangelopoulos, in: R.A. Liss (Ed.), Chemical and Biological Aspects of Vitamin B_6 Catalysis, New York, 1984.
[2] M.A. Spies, M.D. Toney, Biochemistry 42 (2003) 5099.
[3] X. Zhou, M.D. Toney, Biochemistry 38 (1999) 311.
[4] R.A. John, Biochim. Biophys. Acta 1248 (1995) 81.
[5] C.H. Tai, P.F. Cook, Acc. Chem. Res. 34 (2001) 49.
[6] S.N. Smirnov, N.S. Golubev, G.S. Denisov, H. Benedict, P. Schah-Mohammedi, H.H. Limbach, J. Am. Chem. Soc. 118 (1996) 4094.
[7] H.H. Limbach, M. Pietrzak, S. Sharif, P.M. Tolstoy, I.G. Shenderovich, S.N. Smirnov, N.S. Golubev, G.S. Denisov, Chem. Eur. J. 10 (2004) 5195.
[8] S. Sharif, D.R. Powell, D. Shagen, T. Steiner, M.D. Toney, E. Fogle, H.H. Limbach, Acta Crystallogr. B62 (2006) 480.
[9] S. Sharif, D. Schagen, M.D. Toney, H.H. Limbach, J. Am. Chem. Soc. 129 (2007) 4440.
[10] P.E. Hansen, J. Sitkowski, L. Stefaniak, Z. Rozwadowski, T. Dziembowska, Ber. Bunsenges. Phys. Chem. 102 (1998) 410.
[11] Z. Rozwadowski, E. Majewski, T. Dziembowska, P.E. Hansen, J. Chem. Soc. Perkin 2 (1999) 2809.
[12] P. Christen, D.E. Metzler, in: Transaminases, John Wiley, NewYork, 1985.
[13] M. Rospenk, I. Krol-Starzomska, A. Filarowski, A. Koll, Chem. Phys. 287 (2003) 113.
[14] J.C. Zhuo, Magn. Res. Chem. 37 (1999) 259.
[15] (a) Z. Rozwadowski, T. Dziembowska, Magn. Res. Chem. 37 (1999) 274;
(b) Z. Rozwadowski, Magn. Res. Chem. 44 (2006) 881.
[16] L. Kozerski, R. Kawecki, P. Krajewski, B. Kwiecien, D.W. Boykin, S. Bolvig, P.E. Hansen, Magn. Res. Chem. 36 (1998) 921.
[17] T. Dziembowska, Z. Rozwadowski, A. Filarowski, P.E. Hansen, Magn. Res. Chem. 39 (2001) S67.
[18] S.R. Salman, R.D. Farrant, J.C. Lindon, Spectr. Lett. 24 (1991) 1071.
[19] S.H. Alarcon, A.C. Olivieri, M. Gonzalez-Sierra, J. Chem. Soc. Perkin 2 (1994) 1067.

[20] B. Kamienski, W. Schilf, T. Dziembowska, Z. Rozwadowski, A. Szady-Chelmieniecka, Solid State Nucl. Magn. Res. 16 (2000) 285.
[21] S. Sharif, G.S. Denisov, M.D. Toney, H.H. Limbach, J. Am. Chem. Soc. 128 (2006) 3375.
[22] (a) D.M. Blow, J.J. Birktoft, B.S. Hartley, Nature 221 (1969) 337;
(b) D.M. Blow, T.A. Steitz, Annu. Rev. Biochem. 39 (1970) 63;
(c) D. Hadzi, J. Mol. Struct. 177 (1988) 1.
[23] N.S. Golubev, G.S. Denisov, S.N. Smirnov, D.N. Shchepkin, H.H. Limbach, Z. Phys. Chem. 196 (1996) 73.
[24] C.L. Perrin, J.S. Lau, J. Am. Chem. Soc. 128 (2006) 11820.
[25] (a) T. Steiner, W. Saenger, J. Am. Chem. Soc. 114 (1992) 7123;
(b) T. Steiner, W. Saenger, Acta Crystallogr. B50 (1994) 348;
(c) T. Steiner, J. Chem. Soc. Chem. Commun. (1995) 1331;
(d) T. Steiner, J. Phys. Chem. A 102 (1998) 7041;
(e) T. Steiner, Angew. Chem. Int. Ed. 41 (2002) 48.
[26] H.H. Limbach, G.S. Denisov, N.S. Golubev, in: A. Kohen, H.H. Limbach (Eds.), Isotope Effects in the Biological and Chemical Sciences, Taylor & Francis, Boca Raton, 2005.
[27] I.G. Shenderovich, A.P. Burtsev, G.S. Denisov, N.S. Golubev, H.H. Limbach, Magn. Res. Chem. 39 (2001) S91.
[28] N.S. Golubev, I.G. Shenderovich, S.N. Smirnov, G.S. Denisov, H.H. Limbach, Chem. Eur. J. 5 (1999) 492.
[29] J.E. Del Bene, R.J. Bartlett, J. Elguero, Magn. Res. Chem. 40 (2002) 767.
[30] C. Detering, P.M. Tolstoy, N.S. Golubev, G.S. Denisov, H.H. Limbach, Doklady Phys. Chem. 379 (2001) 191.
[31] N.S. Golubev, S.N. Smirnov, P. Schah-Mohammedi, I.G. Shenderovich, G.S. Denisov, V.A. Gindin, H.H. Limbach, J. Gen. Chem. 67 (1997) 1082.
[32] R.W. Layer, Chem. Rev. 63 (1963) 489.
[33] H. Wynberg, E.W. Meijer, Org. Reactions 28 (1982) 1.
[34] (a) H. Benedict, H.H. Limbach, M. Wehlan, W.P. Fehlhammer, N.S. Golubev, R. Janoschek, J. Am. Chem. Soc. 120 (1998) 2939;
(b) S.N. Smirnov, H. Benedict, N.S. Golubev, G.S. Denisov, M.M. Kreevoy, R.L. Schowen, H.H. Limbach, Can. J. Chem. 77 (1999) 943.
[35] P.M. Tolstoy, P. Schah-Mohammedi, S.N. Smirnov, N.S. Golubev, G.S. Denisov, H.H. Limbach, J. Am. Chem. Soc. 126 (2004) 5621.
[36] T. Emmler, S. Gieschler, H.H. Limbach, G. Buntkowsky, J. Mol. Struct. 700 (2004) 29.
[37] H.H. Limbach, M. Pietrzak, H. Benedict, P.M. Tolstoy, N.S. Golubev, G.S. Denisov, J. Mol. Struct. 706 (2004) 115.
[38] G. Zundel, Adv. Chem. Phys. 111 (2000) 1.
[39] N.S. Golubev, G.S. Denisov, V.A. Gindin, S.M. Melikova, S.N. Smirnov, D.N. Shchepkin, in: A.I. Koltsov (Ed.), The Latest NMR Research in Organic and Polymer Chemistry in Russia, Norell Press, Mays Landing, 1996.
[40] M. Ramos, I. Alkorta, J. Elguero, N.S. Golubev, G.S. Denisov, H. Benedict, H.H. Limbach, J. Phys. Chem. A 101 (1997) 9791.
[41] M.J. Mäkelä, T.K. Korpela, Chem. Soc. Rev. 12 (1983) 309.
[42] E.E. Snell, S.J. Di Mari, in: P.D. Boyer (Ed.), The Enzymes, vol. 2, London, 1970.
[43] S. Sharif, G.S. Denisov, M.D. Toney, H.H. Limbach, J. Am. Chem. Soc. 129 (2007) 6313.
[44] T.C. French, D.S. Auld, T.C. Briuce, Biochemistry 4 (1965) 77.